IUST International Journal of Engineering Science, Vol. 17, No.3-4, 2006, Page **53-60**

Experimental Study and Three-Dimensional Numerical Flow Simulation in a Centrifugal Pump when Handling Viscous Fluids

M. H. ShojaeeFard, F. A. Boyaghchi and M. B. Ehghaghi

Abstract: In this paper the centrifugal pump performances are tested when handling water and viscous oils as Newtonian fluids. Also, this paper shows a numerical simulation of the three-dimensional fluid flow inside a centrifugal pump. For these numerical simulations the SIMPLEC algorithm is used for solving governing equations of incompressible viscous/turbulent flows through the pump. The k-ε turbulence model is adopted to describe the turbulent flow process. These simulations have been made with a steady calculation using the multiple reference frames (MRF) technique to take into account the impeller- volute interaction. Numerical results are compared with the experimental characteristic curve for each viscous fluid. The data obtained allow the analysis of the main phenomena existent in this pump, such as: head, efficiency and power changes for different operating conditions. Also, the correction factors for oils are obtained from the experiment for part loading (PL), best efficiency point (BEP) and over loading (OL). These results are compared with proposed factors by American Hydraulic Institute (HIS) and Soviet Union (USSR). The comparisons between the numerical and experimental results show good agreement.

Keywords: Centrifugal pump, Performance, Newtonian fluids, Viscous fluid flow, Correction factors, 3D numerical simulation

1. Introduction

When a fluid of high viscosity –such as heavy oil- is pumped by a centrifugal pump the performance is impaired in comparison to service with water due to increased losses. Viscosity is defined as resistor to pouring with higher viscosity fluids affecting centrifugal pump performance by increasing the power, reducing the flow rate, head and efficiency, making trouble for mechanical seals and causing more load on bearings.

Many researches, such as Daugherty (1926) [1], Stepanoff (1940) [2], Telow (1942) [3], Ippen (1946) [4], and Itaya and Nishikawa (1960) [5], have tested the performance of the centrifugal oil pumps as a function of the viscosity of the viscous oil without knowing the phenomena of viscous fluid flow within the pump. They have proposed some correction factors when pump handles the viscous fluid for determining the performance. These typical results have provided great insights into the effects of the oil viscosity on the performance of centrifugal oil pumps, which have been applied in the important guidelines used today for the design of these pumps. However, these experimental results are based on the oil pump products available in the 1920s and 1950s. On the other hand, some researches, such as Stoffel (1980) [6], Li (1996) [7] and Li and Hu (1997) [8], conducted experiments using commercial centrifugal oil pumps. Theoretical analysis of viscous fluid flow through turbo-machines is impossible or very difficult, and it needs more time for solving the equations by using of super computers. Within the last few years, several computer codes for analyzing the effects of viscosity and boundary layers on turbo machinery performance have been published. The codes use different numerical schemes, boundary conditions and turbulence models for predicting the viscosity effects, impeller tip leakage and secondary flow through blade row. By using this code, Denton

Received by the editor October, 24, 2004; final revised: April, 26, 2006.

M. H. Shojaee Fard and F. A. Boyaghchi are with the Department of Mechanical Engineering, Iran University of Science and Technology Tehran, Iran. mhshf@iust.ac.ir-

M. B. Ehghaghi is a Ph.D. Student at Department of Mechanical Engineering, Tabriz University, ehghaghi@navid.com.

(1986) [9] simulated the viscous effects in the passage of blades by using of a distributed body force. Miner (1992) [10,11] has done several researches on two dimensional flow analysis and turbulence measurements of a centrifugal pump. Croba and Kueny (1996) [12], simulated the 2D, unsteady water flow in centrifugal pump by using the CFD code. Denus and Gode (1999) [13], studied a mixed – flow pump impeller when handling low viscous fluid flow by using the CFD analysis. However, due to the difficulties of the task, most of studies have done heavy simplifications of the problem either in the geometry or in the flow characteristics. Research slowly trends towards more complete simulations. Blanco (2000) [14,15] simulated the fluid flow in the centrifugal pump for investigating the pressure fluctuates in the volute by using the CFD code. Shojaee Fard and Ehghaghi (2002) [16,17] studied the performance of the centrifugal pump experimentally for different geometries of impeller in order to optimizing the centrifugal pump when handling the viscous oil and simulated the fluid flow in a passage of impeller by use of a CFD code. Gugau (2003) [18], simulated the flow in the centrifugal pump by using the sliding meshes for analyzing the main phenomena existent in these pumps. The purpose of the present study is to show a numerical study of a centrifugal pump taking into account the whole 3D geometry of pump which is used in experiments and solving the 3D Navier-Stokes equations using the finite volume method for occurrence of numerical simulation.

2. Experimental Facility

2.1. Test rig

A special centrifugal pump test rig, shown in Figure 1, was used to test the pump performance and to measure the flow within the pump impeller when the pump was pumping viscous oil and water. The pump tested is driven by a three – phase AC electric motor, whose rated power is 5.5 KW and speed is 1450 rev/min.

2.2. Performance Test Method

The pump suction pressure and discharge pressure is measured by a pressure gage. The capacities of the pump are measured by a turbine or nuzzle flow meter. Torque meter measures the shaft torque and speed of the pump. By means of a rotary viscosity meter the viscosity of oil can be given. The density of oil is checked using a floating glass tube density meter.

2.3. Impeller Geometry

The centrifugal pump simulated is a 65-200 single axial suction and vane less volute casing; equipped with an impeller of 209 mm in outside diameter and 6 backwards curved blades. The blade outlet and wrapping angles of the impeller are 27^o and 140^o. When the pump is run at 1450 rev/min the best efficiency point corresponds to 50 m^3/h flow rate and 14 m height. The shroud of the impeller made of metal is machined. The roughness of the impeller and volute is 100 μm. The Figurs 2 and 3 show the impeller configuration and the components of pump respectively.

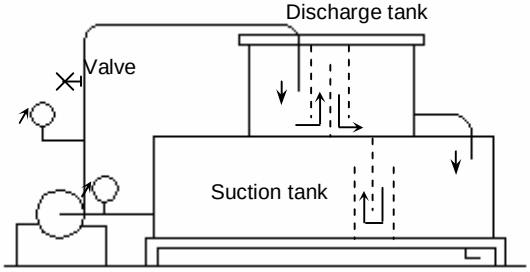

Fig. 1. Centrifugal Pump test Rig

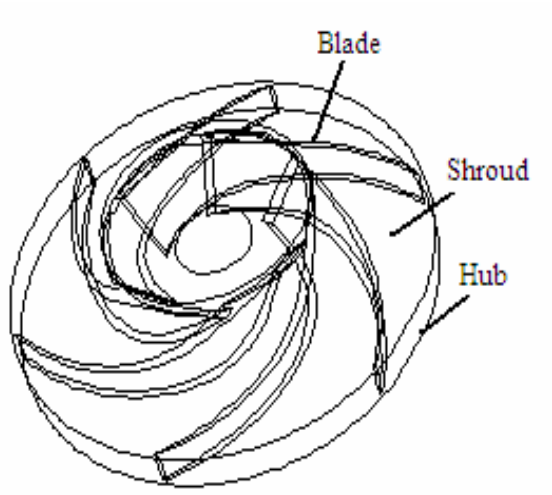

Fig. 2. Impeller Configuration

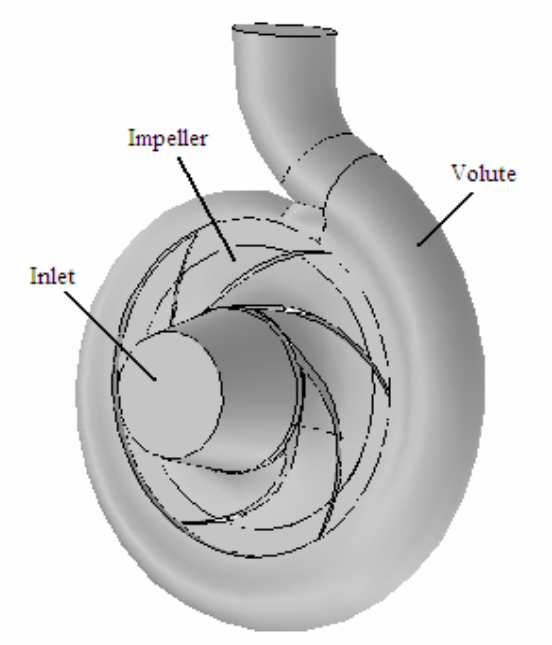

Fig. 3. Components of Pump

2.4. Working Fluid

Working fluids are the special transparent viscous oil refined from crude oils and tap water, respectively.
They are Newtonian fluids verified by using the rotary viscosity meter.
The density and kinematic viscosity of the oils are 875 kg/m^3 and 43×10^{-6} m^2/s and 878 kg/m^3 and 62×10^{-6} m^2/s , respectively, at 20^{o}C.The density and the kinematic viscosity of the tap water are 1000 kg/m^3 and 1×10^{-6} m^2/s, respectively, at 20^{o}C. First, the centrifugal pump performance pump performance and flow fields in the impeller were measured using the tap water as a working fluid. Then the performance and flow fields were measured again using the viscous oils as a working fluid.

2.5. Experimental Uncertainty

The uncertainties in head, capacity, torque, speed and efficiency are 0.4%, 0.5%, 0.3%, 1% and 1.15%, respectively.

3. Model Description and Computational Method

3.1. Pump, Geometry and Grid

With the three-dimensional model there is a useful approach for investigation of flow behavior in different parts of pump.
The blade number and shape has great importance. A pump with few backward blades gives less distortion in the flow and it is possible to simulate it with a relatively rough mesh.
A large number of blades require a great number of cells to correctly simulate the flow passages. Forward blades, because of the severe stall that is usual in the suction side, needs a fine mesh in this area if we want to capture this phenomenon.
Figure 3 shows the unstructured grid generated. There are 45499 cells in the inlet zone, 72591 cells in the impeller and 144206 cells in the volute. This is enough for precise boundary layer simulation and it gives correct values for the pump performance and allows to analysis the details of the main phenomena involved.
Surface between inlet-impeller and impeller-volute correspond to grid interfaces. The multiple reference frame (MRF) technique allows the relative motion of the impeller grid with respect to the inlet and the volute during steady simulation. Grid faces do not need aligned on both sides.

3.2. Mathematical Model

3.2.1. Basic Equations

Continuity and 3-D incompressible Navier-Stokes equations, including the centrifugal force source in the impeller and steady terms are used in centrifugal pump to analyze the turbulent viscous fluid flow.
Turbulence process is simulated with the *k-ε* model. Although grid size is not adequate to correctly take account of boundary layers on blades, wall functions, based on the logarithmic law, has been used. The pressure – velocity coupling is calculated through the SIMPLEC algorithm. Second order, upwind discretizations have been used for convection terms and central difference schemes for diffusion terms.

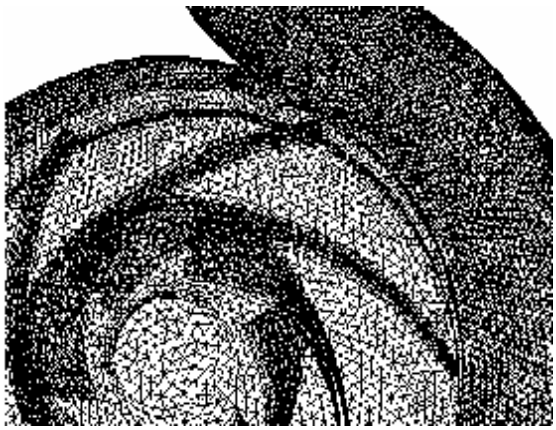

Fig. 4. Sketch of the Pump Grid

The continuity and momentum equations can be written in the rotating coordinate system as follows:

$$\nabla.(\rho U) = 0 \tag{1}$$

and

$$\nabla\cdot(\rho U\otimes U) = \nabla\cdot\left(-P\delta+\mu_{eff}\left(\nabla U+(\nabla U)^T\right)\right)+S_M \tag{2}$$

where vector notation has been used, $\otimes$ is a vector cross- product; U is the velocity; P is the pressure; ρ is the density; δ is the identity matrix; and S_M is the source term.
For flows in a rotating frame of reference that are rotating at the constant rotation speed $\vec{\Omega}$, the effects of the Coriolis are modeled in the code. In this case,

$$S_M = -\rho\left[2\vec{\Omega}\otimes U+\vec{\Omega}\otimes\left(\vec{\Omega}\otimes\vec{r}\right)\right] \tag{3}$$

Where $\vec{r}$ is the location vector.

3.2.2. k-ε Turbulence Model

In Eq. (2), μ_{eff} is the effective viscosity coefficient, which equals the molecular viscosity coefficient, μ, plus the turbulent eddy viscosity coefficient, μ_t:

$$\mu_{eff} = \mu+\mu_t \tag{4}$$

The turbulent viscosity, μ_t, is modeled as the product of a turbulent velocity scale, V_t, and a turbulent length scale, $\mathbf{l}_t$, as proposed by Kolmogorov. Introducing a proportionality constant gives

$$\mu_t = \rho C_\mu \mathbf{l}_t V_t \tag{5}$$

Both equation models take the velocity scale, V_t, to be the square root of the turbulent kinetic energy:

$$V_t = \sqrt{k} \tag{6}$$

The turbulent kinetic energy, k, is determined from the solution of a semi-empirical transport equation. In the standard k-ε two-equation model it is assumed that the length scale is a dissipation length scale, and when the turbulent dissipation scales are isotropic, Kolmogorov determined that

$$e = \frac{k^{3/2}}{\mathbf{l}_t} \tag{7}$$

where e is the turbulent dissipation rate.
Therefore, the turbulence viscosity, μ_t, can be derived from Eq. (5),(6), and (7) to link to the turbulence kinetic energy and dissipation via the relation

$$m_t = C_m r \frac{k^2}{e} \tag{8}$$

where C_μ is a constant. Its value is 0.09.
The values of k, ε come directly from the differential transport equations for the turbulence kinetic energy and turbulence dissipation rate:

$$\nabla.(rUk) - \nabla.(\Gamma_k \nabla k) = p_k - re \tag{9}$$

and

$$\nabla \cdot (rUe) - \nabla \cdot (\Gamma_e \nabla e) = \frac{e}{k}(C_{e1} p_k - C_{e2} re) \tag{10}$$

where the diffusion coefficients are given by

$$\Gamma_e = m + \frac{m_t}{s_e}$$

$$\Gamma_k = m + \frac{m_t}{s_k}$$

and $\sigma_\varepsilon = 1.3$ are constants.
The p_k in Eq. (9) and (10) is the turbulent kinetic energy production term, which for incompressible flow is

$$p_k = m_t \nabla U \cdot (\nabla U + \nabla U^T) - \frac{2}{3}\nabla \cdot U(m_t \nabla \cdot U + rk) \tag{11}$$

Equations (1), (2), (9), and (10) form a closed set of nonlinear partial differential equations governing the fluid motion.

3.2.3. Log-law Wall Function

There are large gradients in the dependent variables near the wall. It is costly to fully resolve the solution in this near-wall region as the required number of nodes would be quite large.
Thus a common approach known as "wall functions" is applied to model this region.
In the wall-function approach the wall tangential velocity is related to the wall shear stress by means of a logarithmic relation, which can be written as follows:

$$u^+ = \frac{1}{k}\ln(y^+) + C \tag{12}$$

Where:

$$u^+ = \frac{u_t}{u_t},$$

$$y^+ = \frac{r \Delta y u_t}{m},$$

$$u_t = \left(\frac{t_w}{r}\right)^{1/2}$$

In above definitions τ_ω is the wall shear stress, u_t is the known velocity tangent to the wall at a distance of Δy from the wall, κ and C are constant depending on wall roughness.
However, this form of the wall-function equations has the problem that it becomes singular at separation points where the near-wall velocity, u_t, approaches zero.
In the logarithmic region, the alternative velocity scale, u^*, can be used instead of u^+:

$$u^* = C_m^{1/4}\sqrt{k} \tag{13}$$

This scale has the useful property of not going to zero if u_t goes to zero (and in turbulent flow, k is never completely zero).
Based on this definition, the following explicit equation for the wall shear stress is obtained:

$$t_w = t_{visc}\frac{y^*}{u^+} \tag{14}$$

Where:

$$t_{visc} = m u_t / \Delta y;\ y^* = r u^* \Delta y / m$$

An estimated of the dissipation consistent with the log-law can be presented as

$$e = \frac{C_m^{3/4}}{k \Delta y} \tag{15}$$

The dissipation at the first interior node is set equal to this value.
The boundary nodal value for k is estimated via an extrapolation boundary condition. The near-wall production of turbulent kinetic energy is derived to be

$$p_k = \frac{t_{visc}^2}{m} p_k^* \quad (16)$$

Where:

$$p_k^* = \left(\frac{y^*}{u^+}\right)\frac{du^+}{dy^+} \quad (17)$$

3.3. Boundary Conditions

At the inlet, a steady, uniform, axial velocity distribution is imposed.

This velocity specifies the flow rate. At the outlet, constant static pressure is maintained.

Non slip boundary conditions have been imposed over the impeller blades and walls, the volute casing and the inlet pipe wall and the roughness of all walls is considered 100 μm. The turbulence intensity at the inlet is totally depends on the upstream history of flow.

Since the fluid in the suction tank is undisturbed, the turbulence intensity for all conditions is considered 1%.

For outlet, the flow is assumed fully turbulent and fully developed. Then the turbulence intensities are estimated by empirical relation blow:

$$I \equiv \frac{u'}{u_{avg}} = 0.16\left(\mathrm{Re}_{DH}\right)^{-1/8} \quad (18)$$

In fully developed duct flows, turbulent length scale is restricted by the size of the duct. An approximate relationship between $\mathbf{l}_t$ and the physical size of the duct is:

$$\mathbf{l}_t = 0.07 D_H \quad (19)$$

Using the above relation, the turbulence length scales at the inlet ($D_{H,in} = 80\,\mathrm{mm}$) and at the outlet ($D_{H,out} = 65\,\mathrm{mm}$) are estimated 5.6 mm and 4.55 mm, respectively.

3.4. Numerical Solution Control

The iterations number has been adjusted to reduce the residual below an acceptable value in each step. The numerical results dependence on the grid size has been tested with a lower number of cells. The overall performance of the pump is the same even with less than a half the cells. Flow main characteristics do not change.

4. Results

4.1. Performance

When a fluid of high viscosity – such as heavy oil- is pumped by a centrifugal pump the performance is impaired in comparison to service with water due to increased losses. The hydraulic losses in the impeller and volute of a centrifugal oil pump include shock loss, diffusion loss and skin friction loss.

The shock and diffusion losses have nothing to do with viscosity, while skin friction losses do.

Table 1 indicates the experimental values of head, efficiency and power for viscous fluids at 20°C. Figure 4 shows the effects of viscosity on the performance of centrifugal pump from experiment.

Table. 1. The Experimental Values of Performance

(a) Water (ν=1×10^{-6} m^2/s)

Flow rate (m^3/h)	0	36	48	60	72	75
Head (m)	15.5	14.3	13.8	12.1	11	10
Power (Kw)	---	2	2.45	2.65	2.8	3.06
Efficiency $(\%)$	0	70	75	76	73	68

(b) Oil (ν=43×10^{-6} m^2/s)

Flow rate (m^3/h)	0	34.9	46.5	58.2	68.8	72.2
Head (m)	14	13.8	13.1	11.6	10.2	9.1
Power (Kw)	---	2.16	2.7	2.9	3.1	3.22
Efficiency $(\%)$	0	47	52	53	50	47

(c) Oil (ν=62×10^{-6} m^2/s)

Flow rate (m^3/h)	0	33.5	44.6	55.8	66.9	69.7
Head (m)	13.8	13.5	12.8	11.1	9.9	8.8
Power (Kw)	---	2.34	2.8	3	3.3	3.6
Efficiency $(\%)$	0	46	49	50	48.2	40.8

4.2. Correction Factor

In order to determine pump performance with viscous oil from known or measured performance with water, it is necessary to establish performance correction factors for the flow rate, head and efficiency as a function of viscosity. The flow rate, head and efficiency correction factors (f_Q, f_H, and f_η) are defined as:

$$f_Q = \frac{Q_u}{Q_w}; \quad f_H = \frac{H_u}{H_w}; \quad f_h = \frac{h_u}{h_w} \quad (20)$$

Where Q_w, H_w, and η_w represent the water flow rate, head, and efficiency at the best efficiency point. Q_υ is the viscous oil flow rate at that point. H_υ and η_υ are the viscous oil head and efficiency under any operating condition. At present there are two series of performance correction factors in use; one is that proposed by the American Hydraulic Institute (HIS) in 1969; the other was formulated by the former Soviet Union (USSR) in the 1950s. Table 2 shows how the correction factors determined in this paper are compared with the two existing sets of factors.

The maximum relative errors ($=\left|\frac{[HIS,USS]_{min}-Experimental}{[HIS,USS]_{min}}\right|$) of the flow rate, head and efficiency correction factors are 2.1%, 2% and 8%, respectively.

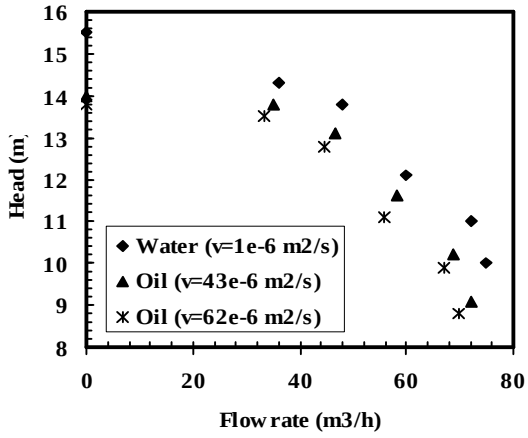

(a)

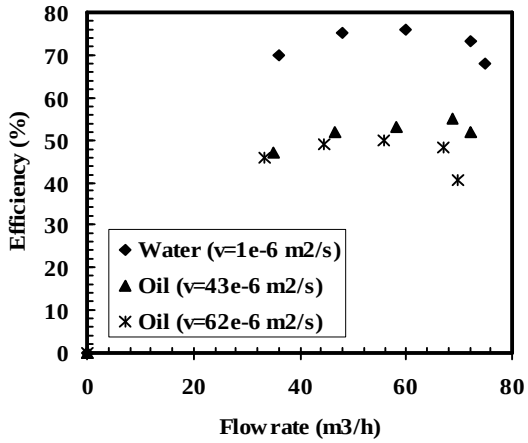

(b)

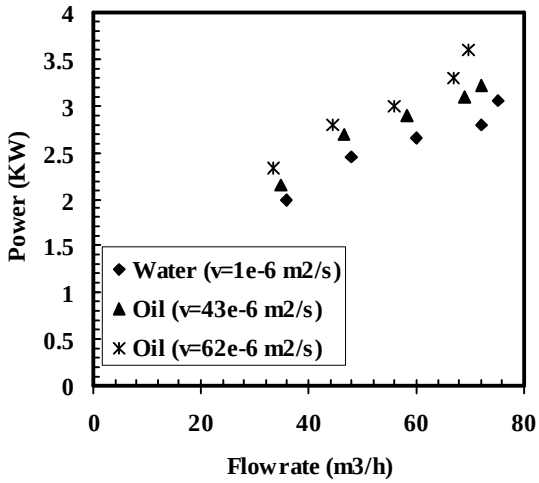

(c)

Fig. 5. The Experimental Effect of Ooil Viscosities on the Performance of Centrifugal Pump in Comparison with Water: (a) Head, (b) Power and (c) Efficiency

4.3. 3D Numerical Results and Comparison with Experiment

For comparison the 3D numerical simulations with experimental head, the BEP points are chosen for different viscosities. Total head is defined as:

$$H=\frac{\Delta P_o}{rg} \tag{21}$$

In equation (21) ΔP_o is the total pressure of outlet and inlet of the pump.

Table 3 shows the values of head obtained using experimental and 3D numerical model.

Table. 2. Comparison of Experimental Results with Existing Correction Factors

Oil , m^2/s		43×10^{-6}	62×10^{-6}
Experimental	f_Q	0.97	0.93
	f_H	0.95	0.91
	f_η	0.69	0.65
HIS	f_Q	0.98	0.95
	f_H	0.96	0.93
	f_η	0.75	0.71
USS	f_Q	0.95	0.92
	f_H	0.97	0.93
	f_η	0.72	0.65

Table. 3. The Comparison of Experimental and Numerical Head for Water and Oils in BEP Points.

Fluid (viscosity,m^2/s)	Experimental head (m)	Numerical head (m)
Water (v= 1×10^{-6})	12.1	11.1
Oil (v=43×10^{-6})	11.6	10.1
Oil (v=62×10^{-6})	11.1	9.5

Figures 6, 7 and 8 show the static pressure contours in BEP (Best Efficiency Point) for various viscous fluids.

For finding the accuracy of 3D model, the numerical simulations were done for different flow rates for each fluid. Figures 9, 10 and 11 show the omparison of experimental head and 3D numerical model for PL, BEP and OL for water and oils, respectively.

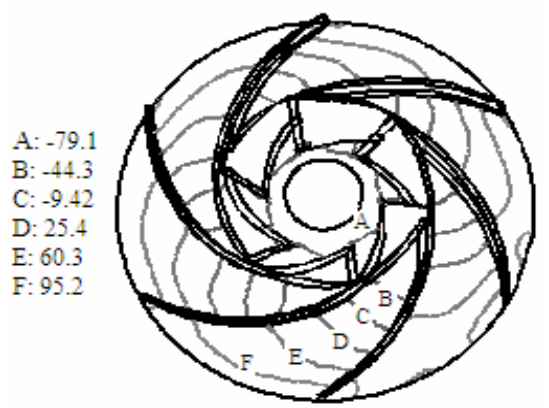

Fig. 6. The Static Pressure (KPa) Ccontours in Impeller when Handling the Water (v=1×10^{-6} m^2/s).

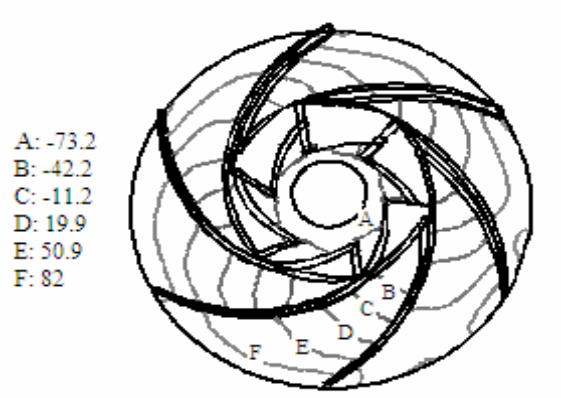

Fig. 7. The Static Pressure (KPa) Contours in Impeller when Handling the Oil (ν=43×10^{-6} m^2/s).

Fig. 8. The Static Pressure (KPa) Contours in Impeller when Handling the Oil (ν=62×10^{-6} m^2/s).

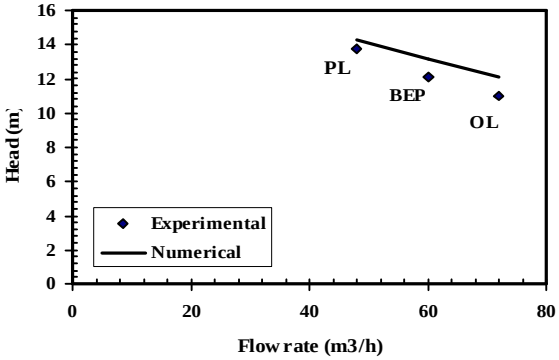

Fig. 9. The Comparison of the Experimental Head with Numerical Model for Water (ν=1×10^{-6} m^2/s).

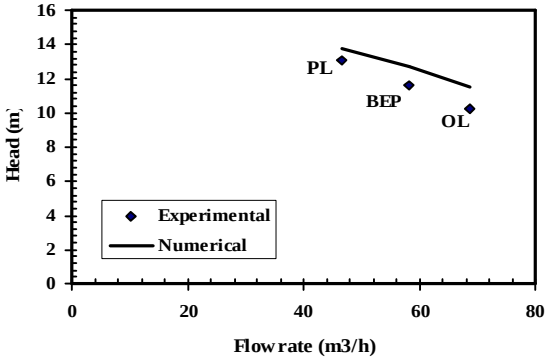

Fig. 10. The Comparison of the Experimental Head with Numerical Model for Oil (ν=43×10^{-6} m^2/s).

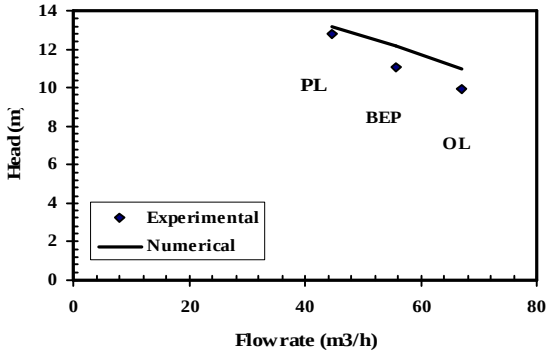

Fig. 11. The Comparison of the Experimental Head with Numerical Model for Oil (ν=62×10^{-6} m^2/s).

5. Conclusion

With regards to the test pump and numerical simulation in the present study the following conclusions can be drawn:

(1) The reason why a centrifugal pump performance goes down when the pump handles high viscosity working fluids is that high viscosity results in a rapid increase in the disc friction losses over outsides of the impeller shroud and hub as well as in hydraulic losses in flow channels of pump.

(2) The head correction factors are related to the pump operating conditions; when determining the performance of liquid with high viscosity from known performance with water, the correction factors must be chosen based on the pump operating conditions.

(3) If the existing correction factors are used to determine the viscous oil performance from known performance in water for current centrifugal oil pumps, the relative errors of up to 8% will occur.

(4) The inlet velocity and pressure outlet conditions can be a good choice for estimating the head of pump after convergence.

(5) The three dimensional view of the pressure over the shroud, blades and part of the volute for the nominal flow point shows that pressure in the hub side is higher than in shroud, due to the transition of flow from the axial to the radial direction. Also, the flow impact over the tongue varies from the center –where the flow comes directly from the impeller- to the sides.

(6) Pressure distribution over the suction and pressure side of the blades when flow rate is the nominal one is clearly appreciated.

(7) Due to this research the numerical simulations with CFD code can be used for investigation of geometrical parameters changes of centrifugal Pump performance for further researches without any vast experimental equipment.

References

[1] Dauherty, R.L., "*A Further Investigation of Performance of Centrifugal Pumps When Pumping Oils*", Bulletin 130, Gould Pumps, Inc., 1926.

[2] Stepanoff, A.J., "*Pumping Viscous Oils with Centrifugal Pumps"*, Oil and Gas Journal, No. 4, 1940.

[3] Telow, N., *"A Survey of Modern Centrifugal Pump Practice for Oilfield and Oil Refinery Services"*, The Institution of Mechanical Engineering, No. 121, 1942.

[4] Ippen, A.T., *"The Influence of Viscosity on Centrifugal Pump Performance*", Trans ASME, pp. 823, 1946.

[5] Itaya, S., and Nishikawa, T., *"Studies on the Volute Pumps Handling Viscous Fluids*", Bulletin of JSME, Vol. 26, No. 162, pp. 202, 1960.

[6] Stoffel, B., *"Tests on Centrifugal Pumps for Handling Viscous Liquids"*, Institute of Chemical Engineers, paper No. 3, 1980.

[7] Li, W.G., *"LDV Measurements and Calculations of Internal Flows in the Volute and Impellers of a Centrifugal Oil Pump"*, Fluids Machinery, Vol. 22, No. 2, 1996.

[8] Li, W.G., and Hu, Z.M. *"An Experimental Study on Performance of Centrifugal Oil Pump*", Fluids Machinery, Vol. 25, No. 2, pp. 3-7, 1997.

[9] Denton, D., "*The use of a Distribution Body Force to Simulate Viscous Effects in 3D flow Calculation*" ASME Journal of Turbo machinery, Vol. 86, GT-144, 1986.

[10] Miner, S.M., "Two Dimensional Flow Analysis of a Laboratory Centrifugal Pump", ASME Journal of Turbo machinery, Vol. 114, 1992.

[11] Miner, S.M., "*Turbulence Measurement in a Centrifugal Pump with a Synchronously Orbiting Impeller"*, ASME Journal of Turbo machinery, Vol. 114, 1992.

[12] Croba, D., and Kueny, J.L., "*Numerical Calculation of 2D, Unsteady Flow in Centrifugal Pumps: Impeller and Volute Interaction"*, International Journal for Numerical Methods in Fluids, Vol. 22, pp.467-481, 1996.

[13] Denus, C.K., and Gode, E., *"A Study in Design and CFD Analysis of a Mixed-Flow Pump Impeller*", ASME-FEDSM-99-6858, 1999.

[14] Blanco, E., *"Numerical Flow Simulation in a Centrifugal Pump with Impeller-Volute Intraction"*, ASME-FEDSM200-11297, 2000.

[15] Blanco, E., *"Numerical Simulation of Centrifugal Pumps*", ASME-FEDSM200-11162, 2000.

[16] Shojaee Fard, M.H., and Ehghaghi, M.B., *"Experimental and Numerical Study of Centrifugal Pump in the Performance of Viscous Flow*", International Journal of Engineering Science, Vol. 13, No. 3, pp. 35-52, 2002.

[17] Shojaee Fard, M.H., and Ehghaghi, M.B., *"Experimental Study of the Increase of Efficiency in Centrifugal Oil Pump*", Ph. D. thesis, Tabriz University of Iran, 2002.

[18] Gugau, M., *"Transient Impeller-Volute Intraction in a Centrifugal Pump*", Technische Universitat Darmstadt, FG Turbomaschinen und Fluidantriebstechnik, 2003.